

the solvent; it even diffuses in rare-gas matrices at 10 K.

The question remains as to what the mechanism is for the release of CO. In the case of the d^6 $M(\text{CO})_4(\alpha\text{-diimine})$ complexes, CO is released for complexes in which the $^3\text{MLCT}$ state is delocalized over the carbonyls in the cis position with respect to the α -diimine ligand.³³ As a result of this delocalization the metal-CO π back-bonding is weakened, and a CO ligand is released. This delocalization of the excited state over the cis carbonyls is reflected in a high relative intensity of $\nu_s(\text{CO})_{\text{cis}}$ in the RR spectra. In the case of the d^8 $M(\text{CO})_3(\alpha\text{-diimine})$ complexes the release of CO could not be explained with a delocalization of the $^3\text{MLCT}$ state over one or more carbonyl ligands. Instead a strong coupling model³⁶ was proposed in which the primary step in solution is the breaking of a metal-nitrogen bond with formation of an intermediate in which the α -diimine ligand is σ -monodentate bound.²³ A nucleophilic ligand then attacks the open site, CO is released and the σ,σ -coordination of the α -diimine ligand is restored again. Although the intermediate could not be identified in the case of the $M(\text{CO})_3(\alpha\text{-diimine})$ complexes, it has been observed for the $(\text{CO})_5\text{MnRe}(\text{CO})_3(\alpha\text{-diimine})$ complexes. We propose the same mechanism for these complexes as for the d^8 $M(\text{CO})_3(\alpha\text{-diimine})$ ones, and this will also be the case for the corresponding $(\text{CO})_5\text{MMn}(\text{CO})_3(\alpha\text{-diimine})$ ($M = \text{Mn, Re}$) complexes in which CO is photosubstituted by 2-MeTHF. The difference in behavior between the two types of complexes is certainly due to the fact that the Re-CO bond is much stronger than the Mn-CO bond. As a result the reaction stops before CO is released in the case of the $(\text{CO})_5\text{MnRe}(\text{CO})_3(\alpha\text{-diimine})$ complexes. When these latter complexes are irradiated with higher energy ($\lambda = 350$ nm), disproportionation into the ions is observed just as in the case of the $(\text{CO})_5\text{MMn}(\text{CO})_3(\alpha\text{-diimine})$ complexes (Figure 11). This wavelength dependence of the reaction is also in agreement with the results for the d^8 $M(\text{CO})_3(\alpha\text{-diimine})$ complexes.^{23,36}

(36) Johnson, C. E.; Troglor, W. C. *J. Am. Chem. Soc.* 1981, 103, 6352.

There is a close relationship between this photochemistry and the mechanisms proposed by McCullen and Brown⁶ and Stiegman and Tyler⁷ for the disproportionation reaction of $\text{Mn}_2(\text{CO})_{10}$ in pyridine. McCullen and Brown proposed a mechanism in which electron transfer takes place from a 17-electron $\cdot\text{Mn}(\text{CO})_3\text{N}_2$ radical to $\text{Mn}_2(\text{CO})_{10}$, whereas Stiegman and Tyler proposed electron transfer from a 19-electron radical with three basic groups, $\cdot\text{Mn}(\text{CO})_3\text{N}_3$. Our experiments show that heterolysis takes place for the $(\text{CO})_5\text{MMn}(\text{CO})_2(\alpha\text{-diimine})(2\text{-MeTHF})$ complexes with three basic donor atoms at one metal fragment and not for the corresponding parent compounds $(\text{CO})_5\text{MMn}(\text{CO})_3(\alpha\text{-diimine})$. This result is in agreement with the mechanism proposed by Stiegman and Tyler.

Acknowledgment. We thank Anja M. F. Brouwers for performing the first experiments leading to this study, Wim de Lange and Henk Gijben for preparing the complexes, Gerard Schoemaker for assistance during the IR experiments, Henk Luiten for making a low-temperature IR cell, Andries Terpstra for assistance during UV experiments, and Dr. Johan Lub for assistance during the ESR experiments.

Registry No. $(\text{CO})_5\text{MnMn}(\text{CO})_3(\text{bpy}')$, 97570-64-4; $(\text{CO})_5\text{MnMn}(\text{CO})_3(\text{phen})$, 60166-19-0; $(\text{CO})_5\text{MnMn}(\text{CO})_3(i\text{-Pr-DAB})$, 71603-98-0; $(\text{CO})_5\text{MnMn}(\text{CO})_3(p\text{-Tol-DAB})$, 71604-00-7; $(\text{CO})_5\text{MnMn}(\text{CO})_3(p\text{-Tol-PyCa})$, 97591-94-1; $(\text{CO})_5\text{ReMn}(\text{CO})_3(\text{phen})$, 61993-44-0; $(\text{CO})_5\text{ReMn}(\text{CO})_3(i\text{-Pr-DAB})$, 97570-65-5; $(\text{CO})_5\text{ReMn}(\text{CO})_3(p\text{-Tol-DAB})$, 97570-66-6; $(\text{CO})_5\text{MnMn}(\text{CO})_2(\text{bpy}')(2\text{-MeTHF})$, 97570-67-7; $(\text{CO})_5\text{MnMn}(\text{CO})_2(\text{phen})(2\text{-MeTHF})$, 97570-68-8; $(\text{CO})_5\text{MnMn}(\text{CO})_2(\text{phen})(P\text{-Bu})_3$, 97570-69-9; $(\text{CO})_5\text{MnMn}(\text{CO})_2(i\text{-Pr-DAB})(2\text{-MeTHF})$, 97570-70-2; $(\text{CO})_5\text{MnMn}(\text{CO})_2(p\text{-Tol-PyCa})(2\text{-MeTHF})$, 97591-95-2; $(\text{CO})_5\text{ReMn}(\text{CO})_2(\text{phen})(2\text{-MeTHF})$, 97570-71-3; $(\text{CO})_5\text{ReMn}(\text{CO})_2(\text{phen})(P(n\text{-Bu})_3)$, 97570-72-4; $(\text{CO})_5\text{ReMn}(\text{CO})_2(i\text{-Pr-DAB})(2\text{-MeTHF})$, 97570-73-5; $(\text{CO})_5\text{ReMn}(\text{CO})_2(i\text{-Pr-DAB})(P(n\text{-Bu})_3)$, 97570-74-6; $(\text{CO})_5\text{ReMn}(\text{CO})_2(p\text{-Tol-DAB})(2\text{-MeTHF})$, 97570-75-7; $\text{Mn}_2(\text{CO})_6(\text{bpy}')_2$, 97570-76-8; $\text{Mn}_2(\text{CO})_6(\text{phen})_2$, 97570-77-9; $\text{Mn}_2(\text{CO})_6(i\text{-Pr-DAB})_2$, 90885-36-2; $\text{Mn}_2(\text{CO})_6(i\text{-Pr-DAB})(2\text{-MeTHF})_2$, 97570-78-0; $\text{Mn}_2(\text{CO})_6(p\text{-Tol-PyCa})(2\text{-MeTHF})_2$, 97570-79-1; $\text{Re}_2(\text{CO})_6(p\text{-Tol-DAB})(2\text{-MeTHF})_2$, 97570-80-4; $\text{Mn}_2(\text{CO})_{10}$, 10170-69-1.

Contribution from the Department of Chemistry, State University of New York at Binghamton, Binghamton, New York 13901

Characterization and Reaction Kinetics of Intermediates Produced in the Photolysis of $M(\text{CO})_6$ ($M = \text{Cr, Mo, W}$) Solutions Containing a 1,4-Diazabutadiene Ligand

MARK J. SCHADT, NANCY J. GRESALFI, and ALISTAIR J. LEES*

Received June 29, 1984

Electronic absorption data have been recorded on a microprocessor-controlled diode-array spectrophotometer at short time intervals following the photolysis of $M(\text{CO})_6$ ($M = \text{Cr, Mo, W}$) in benzene containing 1,4-di-*tert*-butyl-1,4-diazabutadiene (1,4-dab). These spectra illustrate rapid formation of a primary reaction intermediate that is assigned to be a solvent impurity species, $M(\text{CO})_5(\text{impurity})$. This species is then scavenged by ligand to form monodentate $M(\text{CO})_5(1,4\text{-dab})$. UV-visible difference spectra of these reaction intermediates are reported. Rates of formation of $M(\text{CO})_5(1,4\text{-dab})$ have been measured as a function of temperature and ligand concentration. The data imply that $M(\text{CO})_5(\text{impurity})$ is converted to $M(\text{CO})_5(1,4\text{-dab})$ via a dissociative mechanism. Monodentate $M(\text{CO})_5(1,4\text{-dab})$ subsequently extrudes CO by a relatively slow first-order kinetic process to form $M(\text{CO})_4(1,4\text{-dab})$. Rates of chelation for L (ligand) = 1,4-dab are compared with literature values for L = 1,10-phenanthroline and 2,2'-bipyridine and are discussed in terms of the stereochemistry of L when it is coordinated to a metal center in a monodentate fashion.

Introduction

Although a great deal is now known about ligand substitution chemistry of low-valent transition-metal centers, our knowledge of the identity, structure, and reactivity of their reaction intermediates is still very limited. This knowledge is important to a further development of organometallic chemistry. Information about the nature of ligand substitution events at low-valent transition-metal centers is useful in systematic organometallic

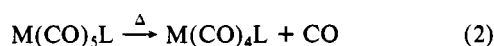
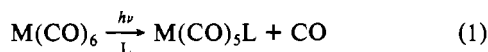
synthesis and in the design of homogeneous catalytic processes. In many of these processes unsaturated species are thought to be involved as reaction intermediates.¹ However, direct spectral evidence for these reaction intermediates and quantitative mea-

(1) (a) Henrici-Olive, G.; Olive, S. "Coordination and Catalysis"; Verlag Chemie: New York, 1977. (b) Geoffroy, G. L.; Wrighton, M. S. "Organometallic Photochemistry"; Academic Press: New York, 1979.

measurements of their reactivity are usually unavailable.

Perhaps the most investigated system has been the $M(\text{CO})_5$ intermediate produced on photolysis of the group 6² hexacarbonyls. Infrared spectra of this intermediate in low-temperature glasses or matrices have shown that its structure is square pyramidal.³⁻⁸ Importantly, it was demonstrated that this species can bind weakly at the vacant coordination site to even poor donors such as rare or hydrocarbon gases in a matrix environment.^{8,9} Conventional flash photolysis and pulse radiolysis experiments have illustrated that in solution the $M(\text{CO})_5$ intermediate is highly reactive toward solvent impurities.¹⁰⁻¹⁴ Recently, laser flash photolysis studies have provided direct spectral evidence for $M(\text{CO})_5$ and shown that it reacts with N_2 , CO , solvent, and $M(\text{CO})_6$, with rate constants approximately at the diffusion limit.¹⁵⁻¹⁷ These studies have also presented kinetic data for the reaction of the solvent-coordinated species.

Chelated complexes of the form $M(\text{CO})_4\text{L}$, where L is a bidentate ligand, are thought to be photochemically formed from $M(\text{CO})_6$ according to the sequence (1)-(2).^{18,19}



In recent years evidence for monodentate $M(\text{CO})_5\text{L}$ has been reported. Staal et al. observed a green transient at -60°C during the substitution reaction of $M(\text{CO})_5(\text{THF})$ ($M = \text{Cr}, \text{Mo}$) with $\text{L} = 1,4$ -diphenyl-1,4-diazabutadiene.²⁰ This species was observed to react rapidly at room temperature to form bidentate $M(\text{CO})_4\text{L}$. Connor et al. have isolated monodentate $M(\text{CO})_5\text{L}$ complexes, where L is a phosphine or arsine derivative, and monitored their chelation reactions by infrared spectroscopy.²¹⁻²³ More recently, monodentate $M(\text{CO})_5\text{L}$ species, where $M = \text{Cr}$ or W and $\text{L} = 4,4'$ -dialkyl-2,2'-bipyridine, have been detected with the use of rapid-scanning Fourier transform infrared spectroscopy.²⁴

In this paper we report on our earlier observation²⁵ of two

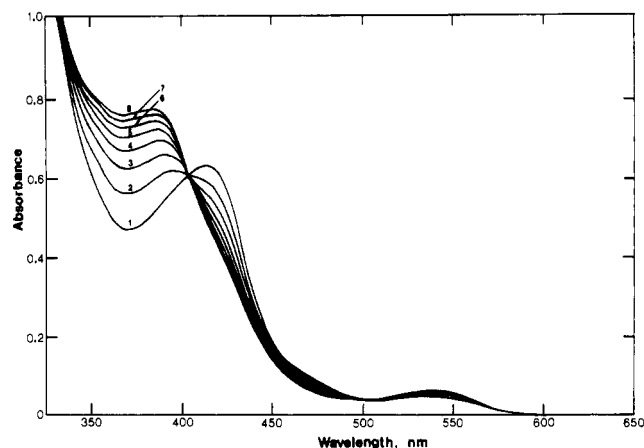
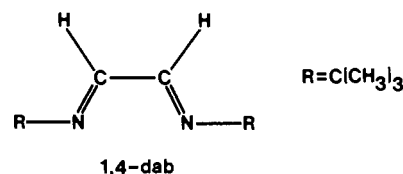


Figure 1. Absorption spectral sequence recorded at 25°C following ~ 2 -s irradiation of a solution of 5×10^{-4} M $\text{W}(\text{CO})_6$ in benzene containing 10^{-2} M 1,4-dab: curve 1, initial spectrum recorded within 4 s after photolysis; curves 2-8, spectra at 15-s time intervals. The spectra illustrate the disappearance of initially produced $\text{W}(\text{CO})_5$ (impurity) to form $\text{W}(\text{CO})_5(1,4\text{-dab})$. The weak absorption at 540 nm is due to a small amount of $\text{W}(\text{CO})_4(1,4\text{-dab})$ produced in the photolysis.

reaction intermediates produced following the photolysis of $M(\text{CO})_6$ ($M = \text{Cr}, \text{Mo}, \text{W}$) with 1,4-di-*tert*-butyl-1,4-diazabutadiene (1,4-dab). Although these intermediates are short-lived, we have



been able to obtain their absorption spectra and determine their reaction kinetics with the use of a rapid-recording microprocessor-controlled diode-array absorption spectrophotometer.

Experimental Section

Materials. The metal hexacarbonyls ($M = \text{Cr}, \text{Mo}, \text{W}$) were purchased from Strem Chemical Co. and used without further purification. Starting materials, *tert*-butylamine and glyoxal, were obtained from Aldrich Chemical Co. Spectroscopic grade benzene (Baker Chemical Co.) was further purified by absorptive filtration through Woelm basic alumina of activity grade 1 (ICN Pharmaceuticals Co.). The nature and extent of impurities in benzene were determined by gas chromatography on a Carle Instruments Co. Model 6500 gas chromatograph equipped with a polar column and by infrared spectroscopy on a Perkin-Elmer 283B spectrometer. The nitrogen used for purging was purified by passage through to 1 m \times 2 cm tubes, the first containing CaSO_4 ($\text{W. A. Hammond Drierite Co.}$) and P_2O_5 (Fisher Scientific Co.) in alternating 20-cm lengths and the second containing a Cu catalyst (BASF R3-11, Chemical Dynamics Corp.). The catalyst was activated prior to use by heating to 120°C while H_2 was passed through the tube. In this form the catalyst effectively removes O_2 from gases. **Caution!** The reduced catalyst is pyrophoric. Other solvents used were reagent grade.

Synthesis of 1,4-dab. *tert*-Butylamine (14.6 g, 0.2 mol) was added to a mixture of distilled water (300 mL) and acetone (50 mL) at 0°C . Aqueous (40%) glyoxal (14.5 g, 0.1 mol) was diluted with distilled water (50 mL) at 0°C and added dropwise to the amine solution while being stirred. Following the addition, the solution was allowed to stand for approximately 2 h at 0°C with occasional stirring. The resulting white crystals were isolated by suction filtration. The product was washed with distilled water and purified by dissolving in anhydrous diethyl ether (50 mL) and discarding the water layer. Evaporation of the ether gave 4.8 g (29% yield) of white crystals, mp $38-40^\circ\text{C}$ (lit.²⁶ mp $39-43^\circ\text{C}$).

Synthesis of $M(\text{CO})_4(1,4\text{-dab})$ Complexes. The complexes were prepared by irradiation of a solution of the parent hexacarbonyl (0.15 mmol) and excess 1,4-dab (0.25 mmol) in isooctane (200 mL) with a 200-W Hg lamp. After 40 min of irradiation the solution was kept at 0°C for 12 h. The product is sparingly soluble in isooctane and precipitates out of solution. Purification was achieved by washing the product several times with isooctane and, if necessary, by column chromatography on 80-200

- (2) In this paper the periodic group notation is in accord with recent actions by IUPAC and ACS nomenclature committees. A and B notation is eliminated because of wide confusion. Groups IA and IIA become groups 1 and 2. The d-transition elements comprise groups 3 through 12, and the p-block elements comprise groups 13 through 18. (Note that the former Roman number designation is preserved in the last digit of the new numbering: e.g., III \rightarrow 3 and 13.)
- (3) Stolz, I. W.; Dobson, G. R.; Sheline, R. K. *J. Am. Chem. Soc.* **1962**, *84*, 3589.
- (4) Stolz, I. W.; Dobson, G. R.; Sheline, R. K. *J. Am. Chem. Soc.* **1963**, *85*, 1013.
- (5) Graham, M. A.; Rest, A. J.; Turner, J. J. *J. Organomet. Chem.* **1970**, *24*, C54.
- (6) Graham, M. A.; Poliakoff, M.; Turner, J. J. *J. Chem. Soc. A* **1971**, 2939.
- (7) Graham, M. A.; Perutz, R. N.; Poliakoff, M.; Turner, J. J. *J. Organomet. Chem.* **1972**, *34*, C34.
- (8) Perutz, R. N.; Turner, J. J. *J. Am. Chem. Soc.* **1975**, *97*, 4791.
- (9) Turner, J. J.; Burdett, J. K.; Perutz, R. N.; Poliakoff, M. A. *Pure Appl. Chem.* **1977**, *49*, 271.
- (10) McIntyre, J. A. *J. Phys. Chem.* **1970**, *74*, 2403.
- (11) Kelly, J. M.; Hermann, H.; Koerner von Gustorf, E. *J. Chem. Soc., Chem. Commun.* **1973**, 105.
- (12) Kelly, J. M.; Bent, D. V.; Hermann, H.; Schulte-Frohlinde, D.; Koerner von Gustorf, E. *J. Organomet. Chem.* **1974**, *69*, 259.
- (13) Nasielski, J.; Kirsch, P.; Wilputte-Steinert, L. *J. Organomet. Chem.* **1971**, *29*, 269.
- (14) Flamigni, L. *Radiat. Phys. Chem.* **1979**, *13*, 133.
- (15) Bonneau, R.; Kelly, J. M. *J. Am. Chem. Soc.* **1980**, *102*, 1220.
- (16) Lees, A. J.; Adamson, A. W. *Inorg. Chem.* **1981**, *20*, 4381.
- (17) Kelly, J. M.; Long, C.; Bonneau, R. *J. Phys. Chem.* **1983**, *87*, 3344.
- (18) Brunner, H.; Herrmann, W. A. *Chem. Ber.* **1972**, *105*, 770.
- (19) Strohmeier, W.; von Hobe, D. *Chem. Ber.* **1961**, *94*, 2031.
- (20) Staal, L. H.; Stufkens, D. J.; Oskam, A. *Inorg. Chim. Acta* **1978**, *26*, 255.
- (21) Connor, J. A.; Day, J. P.; Jones, E. M.; McEwen, G. K. *J. Chem. Soc., Dalton Trans.* **1973**, 347.
- (22) Connor, J. A.; Hudson, G. A. *J. Organomet. Chem.* **1974**, *73*, 351.
- (23) Connor, J. A.; Riley, P. I. *J. Organomet. Chem.* **1975**, *94*, 55.
- (24) Kazlauskas, R. J.; Wrighton, M. S. *J. Am. Chem. Soc.* **1982**, *104*, 5784.
- (25) Schadt, M. J.; Gresalfi, N. J.; Lees, A. J. *J. Chem. Soc., Chem. Commun.* **1984**, 506.

- (26) Kliegman, J. M.; Barnes, R. K. *Tetrahedron*, **1970**, *26*, 2555.

mesh alumina (Fisher Scientific Co.). All samples gave satisfactory chemical (C, H, N) analyses, and their UV-visible absorption spectra agree well with those of the products prepared by thermal procedures.²⁷⁻²⁹ The complexes were reasonably stable in the solid form and were kept in the dark at 0 °C; storing under N₂ effectively increased their long-term stability.

Kinetic Studies. A typical experiment involved ~2-s irradiation of a 3-mL solution of 5×10^{-4} M M(CO)₆ in benzene containing 10⁻² M 1,4-dab. The samples were degassed prior to photolysis by N₂ purging for 15 min. During the irradiation approximately 10⁻⁴ M M(CO)₆ is photodissociated, a value estimated from the reported quantum yields of M(CO)₆³⁰ and the determination of the incident light intensity by ferrioxalate actinometry.³¹ This value was also obtained from the amount of product M(CO)₅L formed. Absorption data were recorded every 1 nm in the 300–400-nm region and every 2 nm in the 400–800-nm region with a microprocessor-controlled diode-array Hewlett-Packard 8450A UV-visible spectrophotometer. The initial spectrum was recorded within 4 s after excitation at 313 nm with an Ealing Corp. 200-W Hg lamp. Spectra were recorded and stored at suitable time intervals thereafter, the shortest interval possible on this equipment being 0.5 s.

Results and Discussion

The UV-visible absorption spectra indicate the rapid formation of a primary reaction intermediate that subsequently forms a relatively long-lived species. The reaction kinetics of the primary and secondary intermediates are discussed independently.

Primary Reaction Intermediate. Figure 1 illustrates the spectral sequence observed following ~2-s photolysis of 5×10^{-4} M W(CO)₆ in rigorously purified benzene containing 10⁻² M 1,4-dab at 25 °C. The primary reaction intermediate ($\lambda_{\max} = 422$ nm) was formed immediately after photolysis during the time needed (≤ 4 s) to record the first spectrum. For M = Cr and Mo the primary species were observed at $\lambda_{\max} = 460$ and 410 nm, respectively, but they were short-lived and we were unable to obtain kinetic data in the 5–50 °C temperature region. The spectral features of the primary species were also observed during photolysis of M(CO)₆ solutions that excluded the 1,4-dab ligand; it is, therefore, considered to be a solvent impurity species, M(CO)₅(impurity).

Considerable effort has been made to identify the nature of this solvent impurity. Infrared spectra of benzene indicated the presence of numerous impurities; among these were sulfur compounds (including thiophene), amines, amides, pyridines, ketones, secondary and tertiary alcohols, carboxylic acids, 1,3,5-trisubstituted benzenes, and phenols. Gas chromatography of benzene determined that several amines and ketones were present in 1–10 ppm (10⁻⁵–10⁻⁴ M) quantities. Electronic absorption spectra of W(CO)₅L, where L is an amine, ketone, sulfur compound, or water, typically yield maxima in the 400–440-nm region, close to the 422-nm value for W(CO)₅(impurity) observed here. Other workers have noted the scavenging of metal carbonyl intermediates at dilute concentrations by solvent impurities and have suggested that the impurity may be an oxygen-containing compound.³² In this vein, we have determined that W(CO)₅(EtOH), W(CO)₅(Et₂O), and W(CO)₅(THF) in benzene absorb with $\lambda_{\max} = 418$, 416, and 420 nm, respectively. In light of the gas chromatography and infrared spectral data, it is concluded that the estimated 0.002 M concentration of solvent impurity present is likely to be an aggregation of several (if not many) oxygen- and nitrogen-containing species. Purification of benzene, as discussed in the Experimental Section, does not completely eliminate the presence of these impurities. It is appropriate to point out that, in identical experiments with scavenging L = 2,2'-bipyridine or 1,10-phenanthroline, the spectral features of M(CO)₅(impurity) were not observable within 4 s following photolysis.²⁵ Therefore, the appearance of M(CO)₅(impurity) illustrates that 1,4-dab is, in comparison to these other diimines, a poor scavenging ligand,

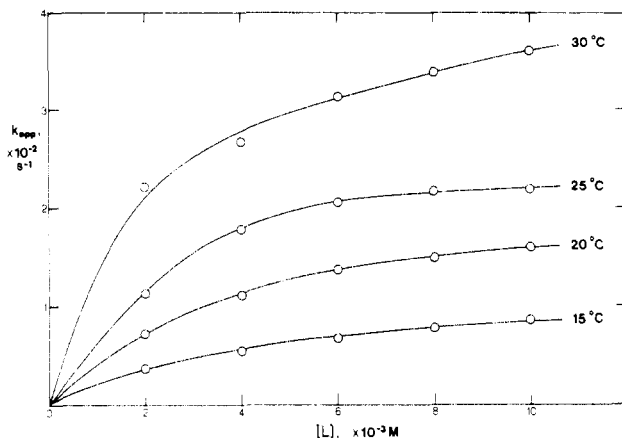
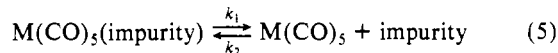
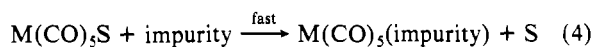
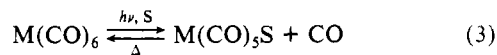


Figure 2. Dependence of the observed first-order rate constant, k_{app} , on 1,4-dab concentration for the reaction of $\sim 10^{-4}$ M W(CO)₅(impurity) with 1,4-dab.

presumably because of steric hindrance by the *tert*-butyl groups around the coordinating nitrogen atom.

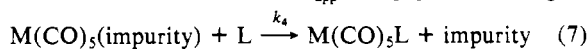
We assign the secondary intermediate to be monodentate M(CO)₅(1,4-dab) on the basis of the spectral and kinetic evidence described below. The growth of A_0 to A_∞ in the 350–390-nm region was exponential; that is, a plot of $\ln [(A_\infty - A_0)/(A_\infty - A_t)]$ vs. time was linear, yielding slope k_{app} . Here, A_0 is the initial absorbance, A_t is the absorbance at time t , and A_∞ is the final absorbance, all absorbance values being recorded at fixed wavelength in this region. Rate constants were also obtained from the absorbance data at wavelengths where the absorbance was decreasing. The reported first-order rate constants reflect the mean of these measurements. Rate constants were obtained for this reaction over a range of ligand concentrations. Plots of k_{app} were linear in 1,4-dab concentration at low values but exhibited saturation at higher ones. This is illustrated in Figure 2 for several temperatures.

The following sequence of reactions is presented to account for our observations:



The initial photoproduct of M(CO)₆ has been determined to be the unsaturated species M(CO)₅S, which rapidly forms a weakly bound solvent complex M(CO)₅S (reaction 3).¹⁴⁻¹⁷ The solvent complex then rapidly scavenges a solvent impurity, forming the primary intermediate M(CO)₅(impurity) (reaction 4), which is the first species observed on our time scale. The primary intermediate decays in the presence of scavenging ligand to form M(CO)₅L (reactions 5 and 6). Recent literature reports indicate that M(CO)₅ will exist as a solvent-coordinated species and that truly "naked" M(CO)₅ is exceptionally short-lived.¹⁴⁻¹⁷

Bimolecular reaction of M(CO)₅(impurity) with 1,4-dab (reaction 7) can be ruled out; here $k_{app} = k_4$, which does not saturate in this mechanism. The variance of k_{app} with [L], shown in Figure



2, instead indicates a dissociative mechanism. Steady-state analysis yields

$$-d[\text{M(CO)}_5(\text{impurity})]/dt = k_{app}[\text{M(CO)}_5(\text{impurity})] \quad (8)$$

$$k_{app} = \frac{K_1 k_3 [\text{L}]}{1 + (k_3 [\text{L}]/k_2')} \quad (9)$$

where

$$K_1 = k_1/k_2' \quad k_2' = k_2[\text{impurity}] \quad (10)$$

(27) Bock, H.; tom Dieck, H. *Angew. Chem.* **1966**, *78*, 549.

(28) Bock, H.; tom Dieck, H. *Chem. Ber.* **1967**, *100*, 228.

(29) tom Dieck, H.; Renk, I. W. *Angew. Chem.* **1970**, *82*, 805.

(30) Strohmeier, W.; von Hobe, D. *Chem. Ber.* **1961**, *94*, 761.

(31) Hatchard, C. G.; Parker, C. A. *Proc. R. Soc. London, A* **1956**, *235*, 518.

(32) Kelly, J. M.; Hermann, H.; Koerner von Gustorf, E. *J. Chem. Soc., Chem. Commun.* **1973**, 105.

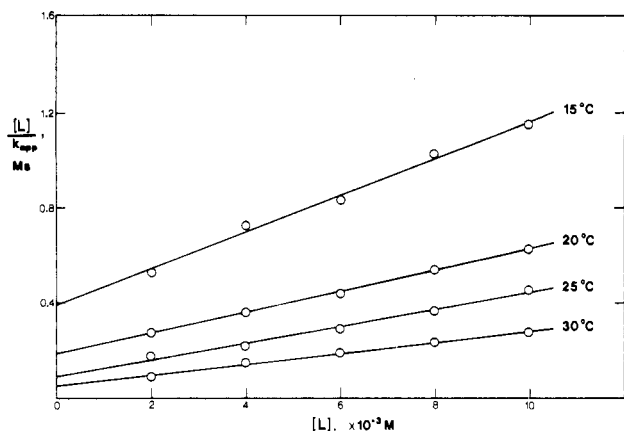


Figure 3. Plots of $[L]/k_{app}$ vs. $[L]$ at 15, 20, 25, and 30 °C for the reaction of $\sim 10^{-4}$ M $\text{W}(\text{CO})_5$ (impurity) with 1,4-dab. $[L]$ is the concentration of 1,4-dab, and k_{app} is the observed rate constant in s^{-1} .

Table I. Temperature Dependence of Derived Rate Constants for the Reaction of $\sim 10^{-4}$ M $\text{W}(\text{CO})_5$ (impurity) with 10^{-2} M 1,4-dab

temp, °C	$10^2 k_1, \text{s}^{-1}$	$10^{-2} k_3/k_2', \text{M}^{-1}$	temp, °C	$10^2 k_1, \text{s}^{-1}$	$10^{-2} k_3/k_2', \text{M}^{-1}$
15	1.29	1.99	25	2.83	3.84
20	2.29	2.35	30	4.32	4.58

Therefore, according to eq 9, a plot of $[L]/k_{app}$ vs. $[L]$ should be linear with slope $1/k_1$ and intercept $k_2'/k_1 k_3$. This relationship does indeed hold; the least-squares lines are illustrated in Figure 3. The calculated k_1 and k_3/k_2' values are shown in Table I. The temperature dependence of these data gave good Arrhenius fits from which we obtained $\Delta H_1^* = 13.3 \text{ kcal mol}^{-1}$ and $\Delta H_3^* - \Delta H_2^* = 10.4 \text{ kcal mol}^{-1}$, the subscripts denoting the corresponding rate constants. The least-squares uncertainty in the above values is $\pm 1.5 \text{ kcal mol}^{-1}$. From the k_1 results, ΔS_1^* was calculated to be $-20.7 (\pm 8) \text{ cal K}^{-1} \text{ mol}^{-1}$. We note that the ΔH_1^* value reflecting the thermal dissociation of impurity from $\text{W}(\text{CO})_5$ (impurity) is close to the 17–28 kcal mol^{-1} range reported for the dissociation of amine from $\text{M}(\text{CO})_5$ (amine)^{33–36} but is considerably less than the activation enthalpies of 39–40 kcal mol^{-1} obtained for the corresponding loss of CO from $\text{W}(\text{CO})_6$,^{36–39} reflecting the weaker metal–ligand bonding. The negative ΔS_1^* calculated supports a transition state with considerable associative character for the forward reaction shown in eq 5. This associative transition state is probably the result of an interaction between a weakly bound solvent molecule and the pentacarbonyl intermediate species.

The software and data storage facilities of the microprocessor-controlled diode-array spectrophotometer enabled us to obtain subtraction spectra readily. Figure 4 illustrates the difference UV–visible absorption spectrum of $\text{W}(\text{CO})_5$ (1,4-dab) obtained by subtracting the spectral data of the unphotolyzed solution from the spectrum recorded 2 min after photolysis. The weak absorption at 540 nm is due to a small amount of $\text{W}(\text{CO})_4$ (1,4-dab) produced in the photolysis. The close similarity of these spectral features to those of $\text{W}(\text{CO})_5$ (pyridine) and $\text{W}(\text{CO})_5$ (piperidine) is strong evidence for the monodentate character of the secondary intermediate.⁴⁰ Absorption data for $\text{Cr}(\text{CO})_5$ (1,4-dab) and $\text{Mo}(\text{CO})_5$ (1,4-dab), summarized in Table II, are also indicative of monodentate coordination.^{41,42} The absorptions of $\text{W}(\text{CO})_5$ -

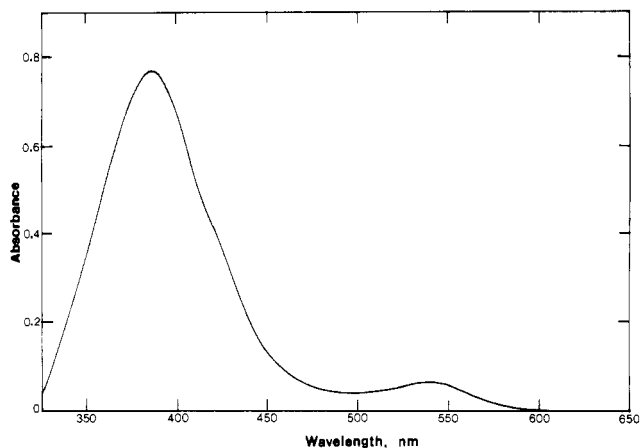


Figure 4. Difference absorption spectrum obtained by subtracting spectral data of the unphotolyzed solution from curve 8 of Figure 1.

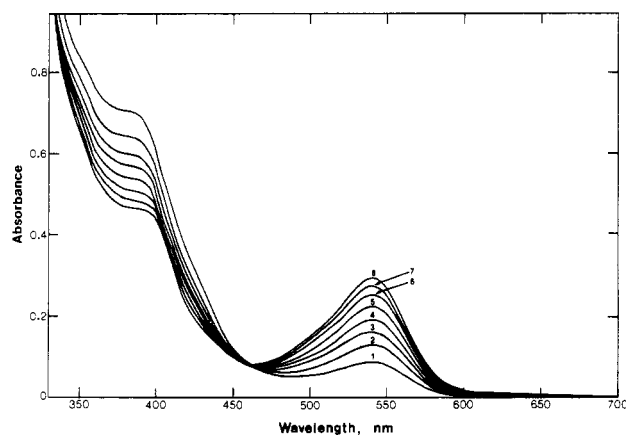


Figure 5. Absorption spectral sequence recorded at 30 °C following ~ 2 -s irradiation of a solution of 5×10^{-4} M $\text{W}(\text{CO})_6$ in benzene containing 10^{-2} M 1,4-dab: curve 1, spectrum recorded 8 min after photolysis; curves 2–8, spectra at 8-min time intervals. The spectra illustrate the disappearance of $\text{W}(\text{CO})_5$ (1,4-dab) to form $\text{W}(\text{CO})_4$ (1,4-dab).

Table II. Electronic Absorption Spectra and Assignments for $\text{M}(\text{CO})_5$ (impurity),^a $\text{M}(\text{CO})_5$ (1,4-dab),^b and $\text{M}(\text{CO})_4$ (1,4-dab)^c Complexes in Benzene at 20 °C

complex	band max, nm	
$\text{Cr}(\text{CO})_5$ (impurity)	460 (d → d)	
$\text{Cr}(\text{CO})_5$ (1,4-dab)	410 (d → d)	
$\text{Cr}(\text{CO})_4$ (1,4-dab)	396 (d → d)	562 (MLCT)
$\text{Mo}(\text{CO})_5$ (impurity)	410 (d → d)	
$\text{Mo}(\text{CO})_5$ (1,4-dab)	380 (d → d)	
$\text{Mo}(\text{CO})_4$ (1,4-dab)	375 (d → d)	532 (MLCT)
$\text{W}(\text{CO})_5$ (impurity)	422 (d → d)	478 (d → d) ^d
$\text{W}(\text{CO})_5$ (1,4-dab)	385 (d → d)	425 (d → d) ^d
$\text{W}(\text{CO})_4$ (1,4-dab)	375 (d → d)	540 (MLCT)

^a Difference spectra obtained from photolysis of 5×10^{-4} M $\text{M}(\text{CO})_6$ in benzene. ^b Difference spectra obtained from photolysis of 5×10^{-4} M $\text{M}(\text{CO})_6$ in benzene containing 10^{-2} M 1,4-dab. ^c Spectra obtained from solutions of the solid complexes. ^d Observed as a shoulder.

(1,4-dab) in benzene at 385 and 425 (sh) nm are therefore assigned to be ${}^1\text{A}(\text{e}^4\text{b}_2^2) \rightarrow {}^1\text{E}(\text{e}^3\text{b}_2^2\text{a}_1^1)$ and ${}^1\text{A}(\text{e}^4\text{b}_2^2) \rightarrow {}^3\text{E}(\text{e}^3\text{b}_2^2\text{a}_1^1)$ ligand-field transitions, respectively. It is noted that the corresponding ${}^1\text{A} \rightarrow {}^3\text{E}$ absorptions are not observable in the spectra of the $\text{Cr}(\text{CO})_5$ (1,4-dab) and $\text{Mo}(\text{CO})_5$ (1,4-dab) complexes, consistent with the spin-forbidden assignment.

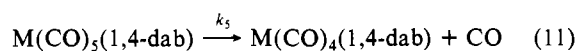
- (33) Darenbourg, D. J.; Brown, T. L. *Inorg. Chem.* **1968**, *7*, 1679.
 (34) Dennenberg, R. J.; Darenbourg, D. J. *Inorg. Chem.* **1972**, *11*, 72.
 (35) Dobson, G. R. *Inorg. Chem.* **1974**, *13*, 1790.
 (36) Graham, J. R.; Angelici, R. J. *Inorg. Chem.* **1967**, *6*, 2082.
 (37) Pajaro, G.; Calderazzo, F.; Ercoli, R. *Gazz. Chim. Ital.* **1960**, *90*, 1486.
 (38) Cetini, G.; Gambino, O. *Atti Accad. Sci. Torino, Cl. Sci. Fis., Mat. Nat.* **1963**, *97*, 757.
 (39) Cetini, G.; Gambino, O. *Atti Accad. Sci. Torino, Cl. Sci. Fis., Mat. Nat.* **1963**, *97*, 1197.
 (40) Wrighton, M. S.; Abrahamson, H. B.; Morse, D. L. *J. Am. Chem. Soc.* **1976**, *98*, 4105.

- (41) Boxhoorn, G.; Schoemaker, G. C.; Stufkens, D. J.; Oskam, A.; Rest, A. J.; Darenbourg, D. J. *Inorg. Chem.* **1980**, *19*, 3455.
 (42) Boxhoorn, G.; Stufkens, D. J.; van de Coolwijk, P. J. F. M.; Hezemans, A. M. F. *Inorg. Chem.* **1981**, *20*, 2778.

Table III. Temperature Dependence of the Observed Rate Constants for the Reaction of $\sim 10^{-4}$ M $M(\text{CO})_5(1,4\text{-dab})$ To Form $M(\text{CO})_4(1,4\text{-dab})$ and CO

M	temp, °C	$10^3 k_5, \text{s}^{-1}$	M	temp, °C	$10^3 k_5, \text{s}^{-1}$
Cr	10	1.21	W	10	0.0136
	20	2.40		20	0.105
	30	7.69		30	0.185
	40	20.0		40	0.463
Mo	10	2.05			
	15	4.18			
	20	6.43			
	25	12.6			
	30	23.8			

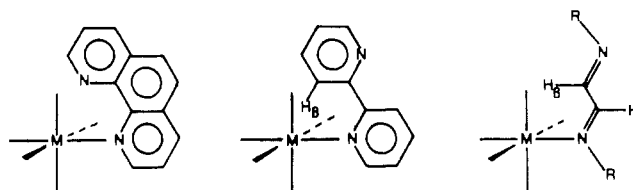
Secondary Reaction Intermediate. The relatively slow thermal reaction of $M(\text{CO})_5(1,4\text{-dab})$ is now considered. Figure 5 illustrates the spectral sequence observed following photolysis at 30 °C of 5×10^{-4} M $W(\text{CO})_6$ in benzene containing 10^{-2} M 1,4-dab. The initial spectrum shown was recorded 8 min after photolysis, at which point it was assumed that the prior formation of $W(\text{CO})_5(1,4\text{-dab})$ was complete. The formation of the reaction product $W(\text{CO})_4(1,4\text{-dab})$ was observed by the growth of its characteristic metal to ligand charge-transfer (MLCT) absorption at 540 nm. The presence of a sharp isosbestic point at 460 nm indicates that this reaction appears to proceed uncomplicated by side or subsequent reactions. The general reaction for the complexes is as follows:



The $M(\text{CO})_4(1,4\text{-dab})$ complexes were also prepared as solid complexes (see Experimental Section), and their spectra are included in Table II. For each metal the spectrum of the isolated complex and the determined A_∞ spectrum were identical, confirming the reaction product.

The rate of reaction 11 was determined by monitoring the decrease of the $d \rightarrow d$ absorption of $M(\text{CO})_5L$ and the corresponding growth in the long-wavelength MLCT feature of $M(\text{CO})_4L$. Reaction rates were found to be independent of ligand concentration over the 1×10^{-3} – 1×10^{-2} M range. The growth of A_0 to A_∞ at long wavelength is exponential, and plots of $\ln [(A_\infty - A_0)/(A_\infty - A)]$ varied linearly with time, yielding slope k_5 . The rate data were recorded at several temperatures; see Table III. From the temperature dependence of the k_5 rate constants, ΔH_5^\ddagger was calculated to be 16.8, 20.4, and 19.7 kcal mol $^{-1}$ for M = Cr, Mo, and W, respectively. The least-squares uncertainty in the above values is ± 1 kcal mol $^{-1}$. The k_5 results yield ΔS_5^\ddagger to be $-12.7 (\pm 8)$, $1.3 (\pm 8)$, and $-10.5 (\pm 8)$ cal K $^{-1}$ mol $^{-1}$, respectively. The relative magnitude of the ΔH^\ddagger and ΔS^\ddagger values illustrates that the enthalpy of activation contributes more to the overall free energy; this observation is consistent with the thermodynamic data obtained by Connor et al. for the slower chelation of $M(\text{CO})_5L$ complexes, where M is Cr, Mo, or W and L is a phosphine or arsine derivative.^{21–23}

It is informative to compare the rate constants and activation energies for dissociation of CO from $M(\text{CO})_5(1,4\text{-dab})$ with the literature values for dissociative loss of CO from the parent hexacarbonyls. For $M(\text{CO})_6$ in solution at 30 °C, rate of CO loss is reported to be 10^{-12} (M = Cr), 5×10^{-10} (M = Mo), and 10^{-14} s $^{-1}$ (M = W),⁴³ substantially slower than the rates obtained here. Similarly, the ranges of reported activation enthalpies for these reactions are 38–40 (M = Cr), 30–32 (M = Mo), and 39–40 kcal

**Figure 6.** Comparison of the stereochemistry of monodentate $M(\text{CO})_5L$ intermediates, where L = 1,10-phenanthroline, 2,2'-bipyridine, or 1,4-diazabutadiene.

mol $^{-1}$ (M = W),^{36–39} considerably greater than our values. Furthermore, the rates of chelation reported here are substantially faster than those observed for thermal substitution of CO in $M(\text{CO})_5L$ complexes in which the entering species is an amine, phosphine, phosphite, or arsenide ligand.^{33,44,45} It is concluded that these differences are brought about by a substantial contribution to the CO extrusion reaction by the associating ligand when it is *already* coordinated in a monodentate fashion.

In contrast to the results for 1,4-dab, the rate of formation of $W(\text{CO})_4(1,10\text{-phenanthroline})$ following photoexcitation of $W(\text{CO})_6$ has been estimated to be >0.2 s $^{-1}$ at 20 °C.²⁵ The factor of $\sim 10^3$ difference is presumably attributable to steric constraints for the bidentate coordination of these diimine ligands; for 1,10-phenanthroline (1,10-phen) the nitrogen atoms are held coplanar in contrast to the *s-trans* conformation of 1,4-diazabutadiene in solution.^{46–51} Furthermore, the $W(\text{CO})_5(1,4\text{-dab})$ intermediate chelates at a significantly slower rate than the corresponding 2,2'-bipyridine (2,2'-bpy) complex.²⁵ These observations can be explained by considering the stereochemistry of L in $M(\text{CO})_5L$. If one assumes that the 1,4-dab and 2,2'-bpy ligands have *s-trans* conformation when initially bound in $M(\text{CO})_5L$, the β -H of L will undergo an appreciable interaction with the CO ligands and metal center. However, because of the geometric positions of the β -H in these molecules, this interaction will be substantially less for 1,4-dab than for 2,2'-bpy (see Figure 6), effectively reducing the stability of the latter monodentate species. The isolation of several monodentate 1,4-dab complexes⁵² in contrast to the absence of corresponding 2,2'-bpy complexes supports this interpretation.

The rate data for the thermal reactions of both $M(\text{CO})_5(\text{impurity})$ and $M(\text{CO})_5(1,4\text{-dab})$ are ordered Mo > Cr > W, consistent with the reactivity of the parent hexacarbonyls.⁴³ This order of lability parallels that of the calculated M–C force constants for $M(\text{CO})_6$ in solution.⁵³

Acknowledgment. We are grateful to the donors of the Petroleum Research Fund, administered by the American Chemical Society, for support of this research.

Registry No. Cr(CO) $_5(1,4\text{-dab})$, 97277-58-2; Cr(CO) $_4(1,4\text{-dab})$, 67033-21-0; Mo(CO) $_5(1,4\text{-dab})$, 97277-59-3; Mo(CO) $_4(1,4\text{-dab})$, 31027-20-0; W(CO) $_5(1,4\text{-dab})$, 91513-50-7; W(CO) $_4(1,4\text{-dab})$, 57304-42-4; 1,4-dab, 30834-74-3; Cr(CO) $_6$, 13007-92-6; Mo(CO) $_6$, 13939-06-5; W(CO) $_6$, 14040-11-0; CO, 630-08-0.

- (44) Ingemanson, C. M.; Angelici, R. J. *Inorg. Chem.* **1968**, *7*, 2646.
 (45) Covey, W. D.; Brown, T. L. *Inorg. Chem.* **1973**, *12*, 2820.
 (46) Nakamoto, K. *J. Phys. Chem.* **1960**, *64*, 1420.
 (47) Cumper, C. W. N.; Ginman, R. F. A.; Vogel, A. I. *J. Chem. Soc.* **1962**, 1188.
 (48) Cureton, P. H.; LeFevre, C. G.; LeFevre, R. J. W. *J. Chem. Soc.* **1963**, 1736.
 (49) Castellano, S.; Gunther, H.; Ebersole, S. *J. Phys. Chem.* **1965**, *69*, 4166.
 (50) Spotswood, T. McL.; Tanzer, C. I. *Aust. J. Chem.* **1967**, *20*, 1227.
 (51) Benedix, R.; Birner, P.; Birnstock, F.; Hennig, H.; Hofmann, H. *J. Mol. Struct.* **1979**, *51*, 99.
 (52) van Koten, G.; Vrieze, K. *Adv. Organomet. Chem.* **1982**, *21*, 151.
 (53) Jones, L. H.; McDowell, R. S.; Goldblatt, M. *Inorg. Chem.* **1969**, *8*, 2349.

(43) Darensbourg, D. J. *Adv. Organomet. Chem.* **1982**, *21*, 113.